LOSING LESS: A LOSS FOR DIFFERENTIALLY PRIVATE DEEP LEARNING

Anonymous authors
Paper under double-blind review

ABSTRACT

Differentially Private Stochastic Gradient Descent, DP-SGD, is the canonical approach to training deep neural networks with guarantees of Differential Privacy (DP). However, the modifications DP-SGD introduces to vanilla gradient descent negatively impact the accuracy of deep neural networks. In this paper, we are the first to observe that some of this performance can be recovered when training with a loss tailored to DP-SGD; we challenge cross-entropy as the de facto loss for deep learning with DP. Specifically, we introduce a loss combining three terms: the summed squared error, the focal loss, and a regularization penalty. The first term encourages learning with faster convergence. The second term emphasizes hard-to-learn examples in the later stages of training. Both are beneficial because the privacy cost of learning increases with every step of DP-SGD. The third term helps control the sensitivity of learning, decreasing the bias introduced by gradient clipping in DP-SGD. Using our loss function, we achieve new state-of-the-art tradeoffs between privacy and accuracy on MNIST, FashionMNIST, and CIFAR10. Most importantly, we improve the accuracy of DP-SGD on CIFAR10 by 4% for a DP guarantee of $\varepsilon = 3$.

1 INTRODUCTION

Releasing machine learning (ML) models may risk the privacy of training data as ML models unintentionally leak information about the training data; this is due to limitations of learning, including overfitting (Song & Shmatikov, 2019) and data memorisation (Fredrikson et al., 2015; Carlini et al., 2019). The framework of Differential Privacy (DP) by Dwork et al. (2014) is the gold standard for formalising privacy guarantees. When training ML models, a DP training algorithm provides guarantees bounding the leakage of private data that may occur during training. This requires that one bound the influence of individual training examples on the output of the algorithm (e.g. parameters or gradients of the model). In addition to these strong theoretical guarantees, DP models are empirically resistant to various attacks – membership inference attacks (Shokri et al., 2017; Rahman et al., 2018), training data extraction (Carlini et al., 2019) and data poisoning attack (Ma et al., 2019).

Differentially Private Stochastic Gradient Descent, DP-SGD, trains a ML model under the framework of DP by (1) clipping per-example gradients to a fixed norm to bound their sensitivity and (2) adding noise to these clipped gradients before they are applied to update the model parameters (Abadi et al., 2016). When done separately and at the level of a minibatch, clipping (Menon et al., 2019; Zhang et al., 2019) or noising (Foret et al., 2021) effectively regularize learning because they respectively control the dynamics of iterates and smoothen the loss landscape. However, gradient clipping and noising are detrimental to model performance in DP-SGD because they are applied in combination and at the granularity of individual training examples. In addition to this, the accuracy of DP-SGD is negatively affected by the limited number of iterations that can be computed: each iteration of DP-SGD increases the privacy budget expended by learning.

Recent works have explored bounded activation functions (Papernot et al., 2021), publicly available feature extractors and data (Tramèr & Boneh, 2021), randomised smoothing (Wang et al., 2021) and gradient embedding (Yu et al., 2021) as a means to improve the tradeoffs between privacy and accuracy of DP-SGD. However, training deep neural networks with strong DP guarantees in DP-SGD still comes at a significant cost in accuracy for datasets like CIFAR10.

In this paper, we show that one key aspect of formulating the optimization problem solved in learning is left out of studies seeking to improve deep learning with DP: the loss function. All existing implementations of deep learning with DP we are aware of optimise cross-entropy (which performs well in the non-privacy-preserving setting with SGD). However, we first observe that optimising cross-entropy with DP-SGD leads to exploding model weights, layer pre-activations and logit values. This is true even if the activation functions themselves are bounded (Papernot et al., 2021). This phenomenon makes it difficult to control the sensitivity of the learning algorithm at a minimal impact to its correctness. Indeed, clipping and noising large gradients in DP-SGD introduces an information loss and additional biases. More precisely, the direction of a minibatch of clipped per-example gradients in DP-SGD is not necessarily aligned with the direction of the original gradients in SGD. Furthermore, we also note that the slow training convergence of cross-entropy (Allen-Zhu et al., 2019) negatively impacts the performance of DP-SGD for which a limited number of iterations are required to achieve strong privacy guarantees.

In this paper, to tackle these two limitations of the cross-entropy loss, we propose to tailor the loss function to the specifics of DP-SGD. We design a novel loss function that takes into account sensitivity, training convergence and the order in which examples are learned with the overarching goal of improving the tradeoffs between privacy and accuracy of DP-SGD. We achieve these objectives with a novel loss function that combines the Sum Squared Error (SSE) between the model logits and ground-truth labels, the focal loss (Lin et al., 2017), and a regularisation penalty on pre-activations.

The first two penalties impose a curriculum structure in the training to improve privacy-accuracy tradeoffs of DP-SGD by exploiting the generalisation and fast convergence speed (Wang et al., 2019; Guo et al., 2018) of curriculum learning (Bengio et al., 2009). We start training with SSE which has faster convergence (Allen-Zhu et al., 2019) and smaller gradients than cross-entropy. Then, we gradually shift toward emphasising hard-to-learn examples using the focal loss: this down-weights gradients assigned to examples that are already learned correctly to focus more on hard-to-learn and misclassified examples. Finally, our regularisation penalty prevents the weights from exploding to further reduce the magnitude of per-example gradients prior to clipping. Implementation-wise, our new loss function can be easily integrated within existing implementations of deep learning with DP; it requires a single line change to edit the loss function being optimized.

In summary, our main contributions are as follows:

- We are the first to investigate the loss function in the context of deep learning with DP. We analyse the effect of the loss function on the sensitivity of DP models by providing extensive analysis of the norm of activations, weights and gradients in Section 4.
- We propose a novel loss function tailored to deep learning with DP. In Section 3 and Section 4, we analytically and experimentally connect the superior performance of our proposed loss function to the gradient norm and direction, smoothness of the loss surface, and convergence of DP-SGD. Our proposed loss function better controls the sensitivity of the learning algorithm by better preconditioning gradients to being clipped and noised.
- We show in Section 4 that our proposed loss function is compatible with other DP-SGD improvement strategies, and more importantly allows us to establish new state-of-the-art tradeoffs between privacy and accuracy on several key benchmarks for deep learning with DP, including CIFAR10. Finally, we perform an ablation study to analyse the effect of each component of our proposed loss function on DP learning.

2 Differential privacy, DP-SGD and state-of-the-art approaches

Trained machine learning models memorise and leak information about their training data (Shokri et al., 2017; Rahman et al., 2018; Song & Shmatikov, 2019; Fredrikson et al., 2015). Differential privacy (Dwork et al., 2014) is the established gold standard to reason about the privacy guarantees of learning algorithms. An algorithm is differentially private if its outputs are statistically indistinguishable on neighbouring datasets. More formally, a randomised learning algorithm A is (ε, δ)-differentially private if the following holds for any two neighbouring datasets D and D' that differ only in one record and all $S \in \text{Range}(A)$:

$$\Pr[A(D) \in S] \leq e^{\varepsilon} \Pr[A(D') \in S] + \delta. \tag{1}$$

The privacy budget ε upper bounds the privacy leakage in the worst possible case: the smaller the ε, the tighter the upper bounds (or stronger privacy guarantee). Note that the factor δ is very small (generally it is chosen to be in the order of the inverse of the dataset size).

In order to train ML models with DP, we can add randomness to the learning algorithm in three ways: output perturbation (Wu et al., 2017; Zhang et al., 2017), objective perturbation (Chaudhuri et al., 2011; Iyengar et al., 2019) or gradient perturbation (Bassily et al., 2014; Abadi et al., 2016). Among these approaches, differentially private stochastic gradient, DP-SGD of Abadi et al. (2016), has established itself as the de facto strategy because of its versatility. DP-SGD perturbs gradients computed at each step of stochastic gradient descent using the Gaussian mechanism to achieve competitive tradeoffs between privacy and accuracy (Yu et al., 2020; Tramèr & Boneh, 2021). Next, we describe the process of training a classifier using DP-SGD on a private dataset.

Let $\mathcal{X} = \{\mathbf{x}_i | i = 1, ..., N\}$ be the training set containing N private examples $\mathbf{x}_i$, and $\mathcal{Y} = \{\mathbf{y}_i | i = 1, ..., N\}$ be the ground-truth label set where each $\mathbf{y}_i$ is a D-dimension one-hot encoded vector. We consider a D-class classifier containing M layers parameterised with weights $\mathcal{W} = \{\mathbf{W}^m | m = 1, ..., M\}$.

In each DP-SGD iteration, similarly to the non-private SGD one, the classifier receives each training example $\mathbf{x}_i$ from a minibatch containing L data points that are sampled randomly from $\mathcal{X}$. The activation of each intermediate layer m of size d_m, $\mathbf{a}_i^m = f(\mathbf{h}_i^m) \in \mathbb{R}^{1 \times d_m}$, is computed by applying a non-linear function, $f(\cdot)$, on the pre-activation $\mathbf{h}_i^m = \mathbf{W}^m \mathbf{a}_i^{m-1}$. The pre-activation is a linear combination of the weight of that layer, $\mathbf{W}^m$, and the activation of the previous layer, $\mathbf{a}_i^{m-1}$. The last layer outputs the logit values associated with each class without any activation function as $\mathbf{a}_i^M = \mathbf{h}_i^M = \mathbf{W}^M \mathbf{h}_i^{M-1} \in \mathbb{R}^{1 \times D}$. The cross-entropy loss, $\mathcal{L}_{\text{CE}}$, for each training example $\mathbf{x}_i$ is computed as

$$\mathcal{L}_{\text{CE}} = -\sum_{d=1}^{D} y_{(i,d)} \log(p_{(i,d)}), \quad \text{where} \quad p_{(i,d)} = \frac{e^{a^M_{(i,d)}}}{\sum_{d'=1}^{D} e^{a^M_{(i,d')}}}. \tag{2}$$

The probability that $\mathbf{x}_i$ belongs to d-th class, $p_{(i,d)} \in [0, 1]$, is computed by applying a Softmax function on the logit value of its corresponding class $a^M_{(i,d)}$.

The DP-SGD optimiser computes *per-example* gradient of $\mathcal{L}_{\text{CE}}$ with respect to $\mathcal{W}$, as opposed to per minibatch gradient in the SGD optimiser, to bound the influence of each individual training example on the output of the learning algorithm (i.e. weight gradients). The gradients, $\mathbf{G}^m$, for each training example $\mathbf{x}_i$ are computed from the last layer and back-propagated until the first layer as:

$$\begin{aligned} \mathbf{G}_i^M &= (\mathbf{p}_i - \mathbf{y}_i)^T \mathbf{a}_i^{M-1}, \quad \mathbf{G}_i^{M-1} = \big((\mathbf{p}_i - \mathbf{y}_i)\mathbf{W}^M\big)^T \mathbf{a}_i^{M-2}, \\ \mathbf{G}_i^{M-2} &= f'\big((\mathbf{p}_i - \mathbf{y}_i)\mathbf{W}^M \mathbf{W}^{M-1}\big)^T \mathbf{a}_i^{M-3}. \end{aligned} \tag{3}$$

One can continue this gradient computation until the first layer. All the per-example gradients are concatenated as $\mathbf{G}_i = [\mathbf{G}_i^1; ...; \mathbf{G}_i^M]$, where ; denotes the concatenation operation. As there is no a priori bound on $\mathbf{G}_i$, the l_2 norm, $\| \cdot \|_2$, of each $\mathbf{G}_i$ are artificially clipped by C to bound the influence of each $\mathbf{x}_i$ on the final gradients, $\mathbf{G}$:

$$\mathbf{G} = \frac{1}{L}\big(\sum_{i=1}^{L} \mathbf{G}_i + \mathcal{N}(0, \sigma^2 C^2 \mathbf{I})\big) \quad \text{where} \quad \mathbf{G}_i \leftarrow \mathbf{G}_i \cdot \min(1, \frac{C}{\|\mathbf{G}_i\|_2}). \tag{4}$$

Finally, the classifier weights are updated through the average of the clipped and noisy (scaled by the noise multiplier σ) per-example gradients of a minibatch.

The accuracy of classifiers trained with DP-SGD is lower than that of classifiers trained by non-private SGD. Recently, researchers investigated the choice of $f(\cdot)$ and data representation for improving the accuracy of the classifier trained by DP-SGD. Papernot et al. (2021) demonstrated that exploiting a bounded family of activation functions instead of the more commonly employed unbounded ReLU activation for the choice of $f(\cdot)$ can decrease the bias introduced by DP-SGD and improve the tradeoffs between privacy and accuracy of DP-SGD. Their approach though does not fully bridge the gap between non-private and private learning for datasets like CIFAR10. Tramèr & Boneh (2021) proposed to train the classifier on a representation of data outputted by a public ScatterNet feature extractor as opposed to using the raw pixels $\mathbf{x}_i$. This however requires access to public data in addition to the private dataset.

3 PROPOSED APPROACH

We propose to design a new loss function tailored to DP-SGD. Our goal is to converge faster with smaller gradient norms, control better the sensitivity of the learning algorithm, increase tolerance to noise, and effectively learn both easy and hard examples. Indeed, these address several crucial differences between DP-SGD and its non-private counterpart SGD:

- Due to per-example gradient clipping (recall Equation 4), information contained in gradients whose magnitude is too large is discarded (see Figure 1.c). This cannot be compensated by tuning the training algorithm, e.g., by increasing the model's learning rate. This is because clipping is done at the granularity of individual training examples. Together with the noise injected (recall Equation 4), this biases learning and implies that DP-SGD takes a different optimisation path compared to SGD.
- As shown in Equation 3, the model weights[1] contribute to the computation of all gradients. In practice, this leads to model weights exploding in DP-SGD. Therefore, one way to decrease the magnitude of gradients is to prevent the model weights from exploding, especially the weight of the last layer which contributes in the gradient of all the layers.
- The number of training iterations are limited in DP-SGD because each iteration increases the risk of privacy leakage. Hence, faster convergence is beneficial to DP-SGD as well as ensuring both easy and hard examples are attended to during the limited training run.

Next, we describe our choice of loss function. We analyse how our new loss function improves the tradeoffs between privacy and accuracy of DP-SGD. We uncover several effects: our loss limits the information loss of gradient clipping, speeds up convergence, recovers a generalisation boost comparable to the one achieved by batch normalisation, and improves learning's tolerance to noise.

3.1 OUR LOSS

We propose to learn the easy examples at the beginning of the training using the per-example Sum Squared Error (SSE) between the logit values and one-hot vector labels:

$$\mathcal{L}_{\text{SSE}} = \frac{1}{2}\|\mathbf{h}_i^M - \mathbf{y}_i\|^2, \quad \text{where} \quad \|\mathbf{h}_i^M - \mathbf{y}_i\|^2 = \sum_{d=1}^{D}(h_{(i,d)}^M - y_{(i,d)})^2. \tag{5}$$

Later in training, we exploit the focal loss $\mathcal{L}_{\text{Focal}}$ to learn hard-to-learn examples. $\mathcal{L}_{\text{Focal}}$ modifies the cross-entropy loss to reduce the loss of easy, well-classified examples, letting the model focus more on hard, misclassified examples. $\mathcal{L}_{\text{Focal}}$ multiplies a factor $(1 - p_{(i,t)})^\gamma$ based on the probability of the ground-truth class $p_{(i,t)}$ to the cross-entropy of each training example $\mathbf{x}_i$ as:

$$\mathcal{L}_{\text{Focal}} = -(1 - p_{(i,t)})^\gamma \sum_{d=1}^{D} y_{(i,d)} \log(p_{(i,d)}), \tag{6}$$

where the tunable focusing parameter γ adjusts the down-weighting rate: the higher the γ, the higher the down-weight rate of easy, well-classified examples. Note that the focal loss is equivalent to cross-entropy loss, when $\gamma = 0$.

To further decrease the gradient magnitudes and prevent the explosion of intermediate weights, we impose a regularisation penalty on the intermediate pre-activations as:

$$\mathcal{L}_{\text{Reg}} = \sum_{m=1}^{M-1} \frac{1}{d_m}\|\mathbf{h}_i^m\|^2. \tag{7}$$

Finally, our proposed loss function $\mathcal{L}$ combines $\mathcal{L}_{\text{Focal}}$, $\mathcal{L}_{\text{SSE}}$ and $\mathcal{L}_{\text{Reg}}$ as:

$$\mathcal{L} = \alpha\mathcal{L}_{\text{Focal}} + (1 - \alpha)\mathcal{L}_{\text{SSE}} + \frac{(1 - \alpha)}{\beta}\mathcal{L}_{\text{Reg}}, \tag{8}$$

where we set hyper-parameter $\alpha = \text{Sigmoid}(e_c - e_t)$ (current epoch, e_c, and threshold epoch, e_t) to enable curriculum learning where easy examples are learned in the early training iterations using $\mathcal{L}_{\text{SSE}}$ which eases learning of hard examples in the later training iterations using $\mathcal{L}_{\text{Focal}}$. We perform a hyper-parameter search to set the best values for α, β and γ.

[1]Note that all the terms except those corresponding to weights are bounded in Equation 3.

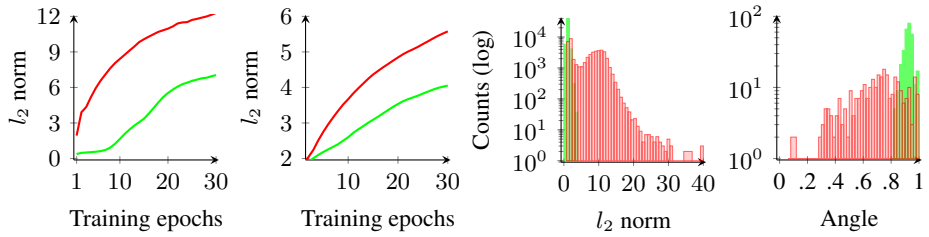

(a) Logit values (b) Weights (c) Gradient (d) Path divergence

Figure 1: l_2 norm of the logit values (a), l_2 norm of the last layer weights (b), histogram of per-sample gradient magnitude in the first epoch (c), and divergence histogram of optimisation path in aggregated clipped gradients from the optimisation path in unclipped ones (d) when we train the classifier on CIFAR10 using cross-entropy loss or our proposed loss function. Minimising cross entropy loss using DP-SGD leads to logit exploding (a) and weight exploding (b). However, our proposed loss function prevents logit exploding (a) and weight exploding (b). Therefore, per-sample gradient magnitudes (c) obtained based on our proposed loss function is smaller than per-sample gradient magnitudes obtained based on cross entropy loss. In addition to this, the per-sample gradients of our proposed loss function is much more condensed. Finally, direction of the gradients (d) of our proposed loss function is more aligned with the unclipped gradients.

3.2 An analysis of our loss

Our loss limits information loss from clipping. Figure 1 shows that under the supervision of $\mathcal{L}$, we are able to control the sensitivity of the learning algorithm. In particular, we prevent logit values and weights from exploding, which decreases the magnitude and variance of per-example gradients (see Equation 3). Smaller and more condensed gradients decrease the negative impact of gradient clipping on the trajectory of the gradient descent as shown in Figure 1.d.

Our loss yields faster convergence. $\mathcal{L}_{\text{SSE}}$ improves the tradeoffs between privacy and accuracy of DP-SGD with strong privacy budgets as $\mathcal{L}_{\text{SSE}}$ converges exponentially $O(e^{-t})$, where t is the steps, to 0 loss, while cross-entropy loss only converges at $O(1/t)$ as shown in Allen-Zhu et al. (2019).

Our loss achieves an effect similar to batch normalisation. The magnitude of gradients computed when optimising $\mathcal{L}_{\text{SSE}}$ with DP-SGD is smaller than for gradients computed when optimising cross-entropy, as $\mathcal{L}_{\text{SSE}}$ is defined on logit values $\mathbf{h}_i^M$. This prevents logit values and consequently $\mathbf{W}^M$ from exploding (per-example logit values are computed based on the weight of the last layer). Controlling $\mathbf{W}^M$ can limit the changes of weights in other layers as their gradients are a function of $\mathbf{W}^M$ and per layer gradient function is locally lipschitz. Preventing logits from exploding may also help recover the generalisation boost of batch normalisation (Dauphin & Cubuk, 2021). Indeed, batch normalisation cannot be used in differentially private learning because the technique shares information across different training examples contained in a single minibatch. This violates the privacy analysis of DP-SGD. Therefore, our proposed $\mathcal{L}_{\text{SSE}}$ penalty may also be beneficial to learning with DP-SGD because it achieves a similar effect to batch normalisation (Dauphin & Cubuk, 2021).

Our loss improves tolerance to noise. Wang et al. (2021) showed that smoother loss functions improve the generalisation bounds and accuracy of DP learning by making the loss surface more tolerant to noise. The most common smoothness notion is based on the Lipschitz constant of the gradient of a function.

Definition 1 (Smoothness (Nesterov, 2003)) *A loss function $\mathcal{L}$ is β-smooth if*

$$\|\nabla\mathcal{L}_w - \nabla\mathcal{L}_{w'}\|_2 \leq \beta\|w - w'\|_2,$$

where $\nabla\mathcal{L}_w$ is the gradient of the loss function with respect to the weights and β is the smoothness constant. Smaller β indicates a smoother function.

We now derive a lemma illustrating how our loss also favours smoothness of the loss being optimised by DP-SGD.

Lemma 1 *When singular values are bounded by σ_{max}, we have for all w and w' in a simply connected set that $\|\nabla\mathcal{L}_w - \nabla\mathcal{L}_{w'}\|_2 \leq \sigma_{max}\|w - w'\|_2$.*

Proof.
Let H_w be the hessian of the loss function with respect to the weights w.

$$\|\nabla\mathcal{L}_w - \nabla\mathcal{L}_{w'}\|_2 = \|(\int_0^1 H_{w+t(w-w')} \cdot (w - w')dt)\|_2 \leq \int_0^1 \|H_{w+t(w-w')} \cdot (w - w')\|_2 dt$$
$$\leq \int_0^1 \sigma_{max}\|w - w'\|_2 dt \leq \sigma_{max}\|w - w'\|_2, \tag{9}$$

where σ_{max} is the maximum of the first singular value along the line from w to w'.

Therefore, the existence of local bounds on the singular values results in local bounds on the smoothness. We empirically observe in Figure 2 that the singular values of our loss function are smaller than cross-entropy loss function. This is particularly true at the beginning of training. This, thus, suggests that our proposed loss function is smoother and more noise-tolerant than cross-entropy.

4 VALIDATION

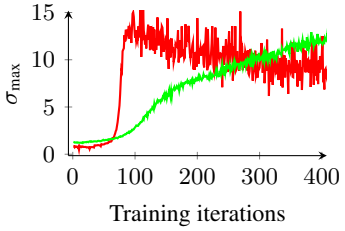

Figure 2: Analysing the smoothness of the landscape of our proposed loss function and cross-entropy on MNIST. Our loss function obtains smaller $\sigma_{\max}$ (the maximum of the first singular value), making it more smooth than cross entropy.

We validate the benefit of deploying our proposed loss function in improving how DP-SGD tradeoffs privacy and accuracy. To do so, we show our loss further improves the state-of-the-art results of the two approaches for deep learning with DP described in Section 2–1) `CE-T-CNN` (Papernot et al., 2021): using the cross-entropy loss function together with an end-to-end CNN classifier equipped with Tanh activation functions; 2) `CE-T-PFE_CNN` (Tramèr & Boneh, 2021): using the cross-entropy loss function, this time combining the ScatterNet public feature extractor (PFE) with a private CNN classifier whose internal activations are also Tanh. To ensure a fair evaluation, we use the same datasets, MNIST, FashionMNIST and CIFAR10, and the same classifiers (described in Appendix A) as these two baseline approaches. In addition to this, we fix the DP-SGD configuration across all approaches to the best hyperparameter values reported in the hyperparameter search done by Tramèr & Boneh (2021) (see Appendix B). Note that our results would only be improved by additional hyperparameter search on the DP-SGD configuration. For the hyperparameters introduced by our own loss function, we use a search on the values as described in detail in Appendix B. We note that none of the prior work we compare against captures the privacy cost of the hyperparameter search itself when reporting DP guarantees achieved. The cost of this search should however be moderate, as analysed by Liu & Talwar (2019).

4.1 IMPROVING THE TRADEOFFS BETWEEN PRIVACY AND ACCURACY

Figure 3 and 4 compare the privacy-accuracy tradeoffs achieved by our proposed loss function and prior approaches for DP training. Coloured regions represent the range of model accuracy with respect to the privacy budget ε needed to achieve this accuracy. Experiments are repeated 5 times; the minimum, median and maximum of the 5 experiments are each highlighted by a line.

When learning without privacy, end-to-end classifiers achieve a test accuracy on CIFAR10, FashionMNIST and MNIST of 76.6%, 89.4% and 99.0%, respectively. Instead, when learning with DP-SGD, the maximum test accuracy (across 5 runs) of our first baseline `CE-T-CNN` for $\varepsilon < 3$ are 59.8%, 86.9%, 98.2% on CIFAR10, FashionMNIST and MNIST, respectively. This illustrates how CIFAR10 is the most challenging dataset for DP-SGD training among the datasets we considered: there is about 20% gap in accuracy between the privacy-preserving and non-privacy-preserving settings. Our proposed loss function reduces this gap significantly, even more so for CIFAR10 than simpler datasets like FashionMNIST and MNIST. For example, training an end-to-end classifier

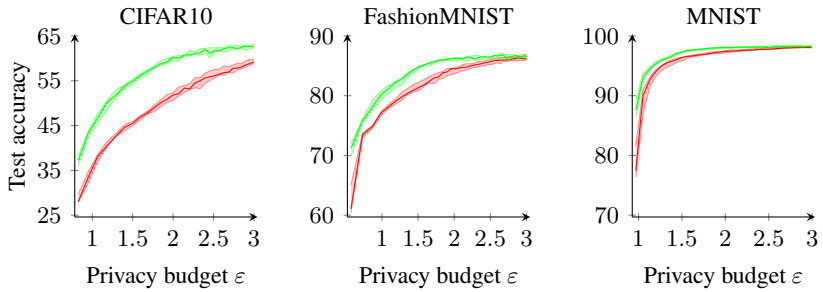

Figure 3: Deployment of our loss function in DP-SGD training of a end-to-end classifier for 5 runs. Comparison between the test accuracy of CE−T−CNN (Papernot et al., 2021) (——) and O−T−CNN, ours (——), as a function of privacy budget ε.

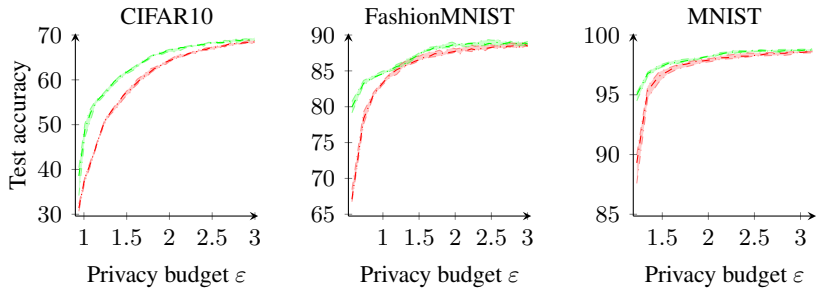

Figure 4: Deployment of our loss function in DP-SGD training of a public feature extractor followed by a classifier for 5 runs. Comparison between the test accuracy of CE−T−PFE_CNN (Tramèr & Boneh, 2021) (-·-·-) and O−T−PFE_CNN, ours (-·-·-), as a function of privacy budget ε.

using our loss function on CIFAR10 achieves 63.2% test accuracy, instead of 59.8% with the cross-entropy loss. While our second baseline CE−T−PFE_CNN sees stronger accuracy than the first baseline CE−T−CNN because the learner additionally has access to public data, our proposed loss function also improves its ability to tradeoff privacy and accuracy across the entire ε regime.

The improvement of our proposed loss function to privacy-accuracy tradeoffs is strongest in the initial epochs. These epochs correspond to stronger privacy guarantees (i.e., smaller values of ε) because the privacy guarantee of each individual step of DP-SGD needs to be composed across the entire training run; hence each step further increases the privacy budget expended. For example, our proposed O−T−CNN trains an end-to-end classifier with 55.4% test accuracy for $\varepsilon < 1.5$, compared to 45.9% only with our first baseline CE−T−CNN. In another example, O−T−PFE_CNN improves the test accuracy of our second baseline CE−T−PFE_CNN from 64.5% to 66.8% for $\varepsilon < 2$.

4.2 Analysis of Gradients computed by DP-SGD for O−T−CNN

We first analyse the impact of the loss function on the model weights, pre-activations, and logit values. Figure 5 (first row) shows the impact our loss function has on **model weights**. We visualise the average l_2 norm of model weights at each epoch. Across the three datasets, optimising CE−T−CNN with DP-SGD leads to model weight explosion. This is not the case when learning with our proposed loss. In particular, note how O−T−CNN prevents last layer weights from exploding, which is important because they contribute to the gradients for all layers. Next, Figure 5 (second row) shows the impact of our loss function on **pre-activation and logit norms**. Although CE−T−CNN uses bounded tanh activation functions to prevent activations from exploding, the pre-activations and logits still explode because model weights are unbounded and explode themselves (as visualized above). Instead, replacing the cross-entropy loss function with our loss function decreases this phenomenon for both pre-activations and logits. This is explained by our pre-activation regulariser penalty but also the fact that the sum-squared-error penalty is defined over logits.

Reducing the bias of gradient clipping. We provide the histogram of per-example gradient l_2 norms in Figure 6. For better visualisation, we clip the x-axis between $[0, 100]$ and use a log scale for the y-axis. The gradient l_2 norms of O−T−CNN are smaller than their counterpart for CE−T−CNN. This is a consequence of our observations above: our proposed loss function prevents several terms

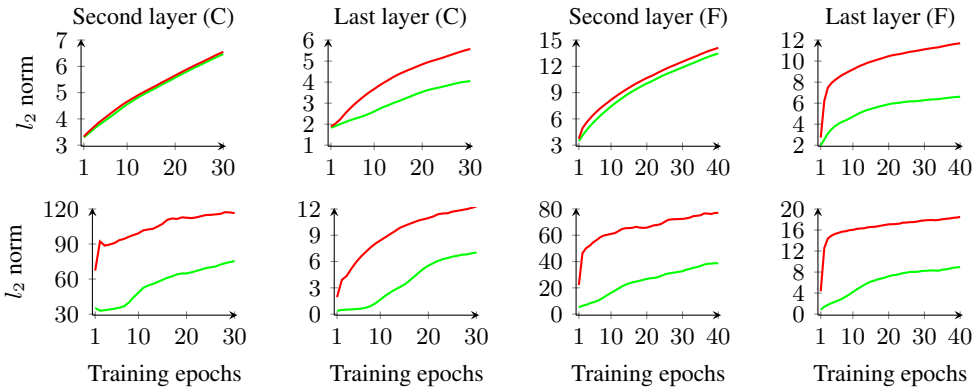

Figure 5: l_2 norm of weights (first row) and pre-activations (second row) in CE−T−CNN (——) and O−T−CNN (——) using CIFAR10 (C) and FashionMNIST (F). See Appendix C for results of MNIST and other layers.

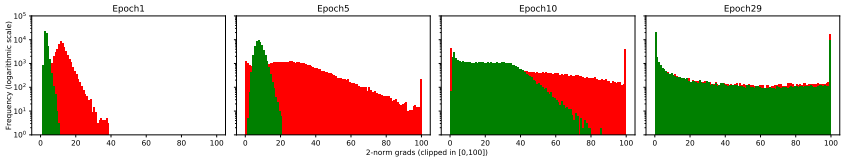

Figure 6: Histogram of l_2 norm of per-example gradient in CE−T−CNN and O−T−CNN on CIFAR10. Histogram for other epochs and other datasets are presented in Appendix E.

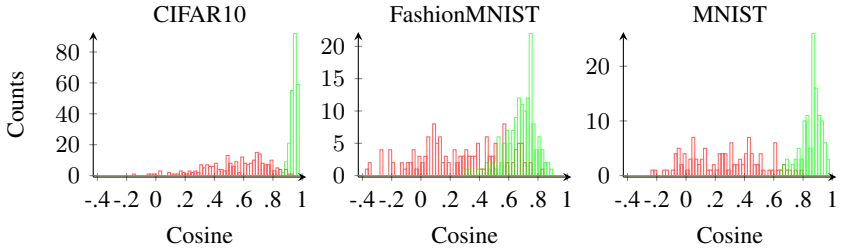

Figure 7: Cosine similarity between aggregated of clipped per-example gradients and aggregated of unclipped per-example gradients in first epoch of CE−T−CNN (——) and O−T−CNN (——).

including in the gradient computation from exploding. To further demonstrate the importance of better preconditioning gradients to the clipping performed by DP-SGD, we visualize the divergence between the path taken by aggregated *clipped* per-example gradients and aggregated *unclipped* per-example gradients in Figure 7. For each minibatch, we compute the cosine similarity between the average of per-example clipped gradients and the average of per-example unclipped gradients. The direction of clipped gradients in O−T−CNN is more aligned with the direction of their unclipped counterparts than is the case for the baseline approach. This suggests that our proposed loss function decreases the information loss and bias introduced by DP-SGD.

Learning hard vs. easy examples. Finally, we visualise the confusion matrices of per-class training accuracy for non-private learning with SGD, private learning with the CE−T−CNN baseline, and private learning with our approach O−T−CNN in Figure 8. Qualitatively speaking, the per-class training accuracy of O−T−CNN is closer to the non-private one than is the case for the baseline CE−T−CNN. During the initial epochs of learning, O−T−CNN converges faster especially on easy-to-learn examples thanks to the sum-squared-error loss function. For example, the training accuracy of O−T−CNN for "car" and "truck" are 51% and 48%, while CE−T−CNN only achieves 34% and 37%, respectively, on these classes. In addition to this, O−T−CNN deals better with hard-to-learn examples (e.g. "cat", "dear" or "dog" classes) in later epochs thanks to the focal loss. For example, the training accuracy of "cat" class is 49% at epoch 20 of O−T−CNN, but is only 35% for CE−T−CNN.

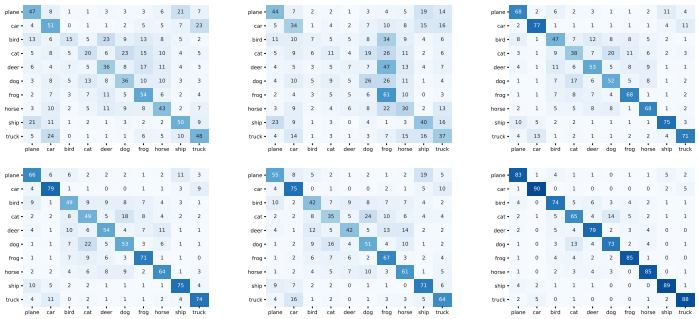

Figure 8: Confusion matrices that show per-class training accuracy of O−T−CNN (first column), CE−T−CNN (second columns) and non-private SGD approach (last columns). The first and second row show confusion matrices of CIFAR10 at epoch 2 and 20, respectively. See Appendix D for the results of other epochs as well as FashionMNIST and MNIST datasets.

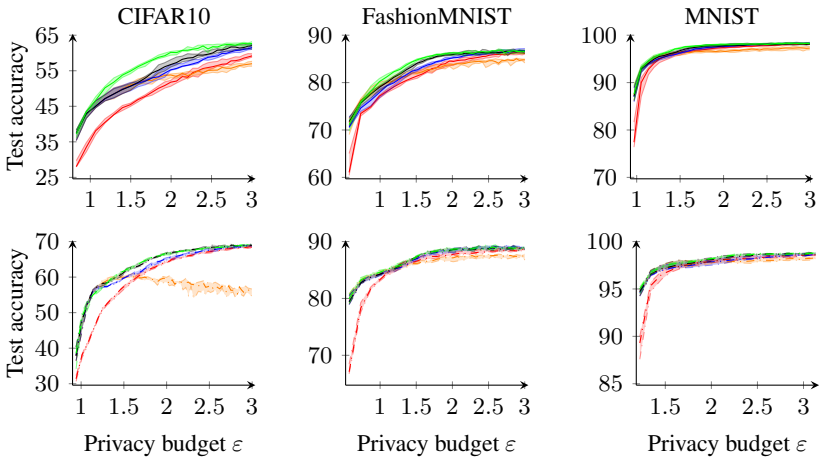

Figure 9: Ablation study of DP-SGD training of an end-to-end classifier (first row) and a public feature extractor followed by a classifier (second row) for 5 runs. Loss functions under study: CE, SSE, SSE+CE, SSE+Focal and SSE+Focal+Regulariser.

4.3 Ablation Study

Next, we present an ablation study to tease out the contribution of each of the three components of our proposed loss when it comes to improving privacy-accuracy tradeoffs in deep learning with DP, namely sum-squared-error, focal loss and regularisation penalty. To do that we consider four combinations of these penalties: only using sum-squared-error, a combination of sum-squared-error and cross-entropy, a combination of sum-squared-error and focal loss, and finally our proposed loss function that combines all three-sum-squared-error, focal loss and regulariser. We do not consider other combinations because they are not meaningful. To ensure a fair evaluation, we perform a hyperparameter search for the combination of sum-squared-error and cross-entropy as well as the combination of sum-squared-error and focal loss, similarly to the search performed for our proposed loss function (see Appendix B). The privacy-accuracy tradeoffs of these four combinations is shown in Figure 9. While the sum-squared-error improves the privacy-accuracy tradeoff in initial epochs, the focal loss improves it for later epochs. Finally, imposing a regularisation penalty on pre-activations further improves these privacy-accuracy tradeoffs. Our proposed loss thus achieves the best possible performance across each of these settings and none of its penalties can be omitted.

5 Conclusion

In this paper, we showed that designing a loss function tailored to the specificities of DP-SGD, namely per-example gradient clipping and a limited number of iterations, significantly improves tradeoffs between privacy and accuracy. We reduced the bias introduced by gradient clipping using a pre-activation regularisation term. In addition to this, we improved the convergence speed by imposing a curriculum structure in learning with the sum-squared-error and focal loss. As future work, we will evaluate our loss function for DP-SGD in other domains such as text.

6 REPRODUCIBILITY STATEMENT

We submit our code as the supplementary material. Our code is based on the public Opacus library in PyTorch. We use the publicly available datasets. For the theoretical smoothness result, we provide clear explanations of lemma and complete proof.

7 ETHICS STATEMENT

Our work improves the tradeoffs between privacy and accuracy of training machine learning models in privacy-preserving setting. Therefore, we expect the broader impact of our work to be generally positive especially in privacy-sensitive applications such as health-care or language modeling where we work with sensitive datasets in practice.

REFERENCES

Martin Abadi, Andy Chu, Ian Goodfellow, H Brendan McMahan, Ilya Mironov, Kunal Talwar, and Li Zhang. Deep learning with differential privacy. In *Proceedings of the ACM SIGSAC Conference on Computer and Communications Security (CCS)*, Vienna, Austria, October 2016.

Zeyuan Allen-Zhu, Yuanzhi Li, and Zhao Song. A convergence theory for deep learning via over-parameterization. In *Proceedings of the International Conference on Machine Learning (ICML)*, Long Beach, California, USA, June 2019.

Raef Bassily, Adam Smith, and Abhradeep Thakurta. Private empirical risk minimization: Efficient algorithms and tight error bounds. In *Proceedings of the IEEE Symposium on Foundations of Computer Science (FOCS)*, Washington, USA, October 2014.

Yoshua Bengio, Jérôme Louradour, Ronan Collobert, and Jason Weston. Curriculum learning. In *Proceedings of the International Conference on Machine Learning (ICML)*, Montreal Quebec, Canada, June 2009.

Nicholas Carlini, Chang Liu, Úlfar Erlingsson, Jernej Kos, and Dawn Song. The secret sharer: Evaluating and testing unintended memorization in neural networks. In *Proceedings of the USENIX Security Symposium*, Santa Clara, California, USA, August 2019.

Kamalika Chaudhuri, Claire Monteleoni, and Anand D Sarwate. Differentially private empirical risk minimization. *Journal of Machine Learning Research (JMLR)*, 12(3):1069–1109, 2011.

Yann Dauphin and Ekin Dogus Cubuk. Deconstructing the regularization of BatchNorm. In *Proceedings of the International Conference on Learning Representations (ICLR)*, Virtual, May 2021.

Cynthia Dwork, Aaron Roth, et al. The algorithmic foundations of differential privacy. *Foundations and Trends in Theoretical Computer Science*, 9(3-4):211–407, 2014.

Pierre Foret, Ariel Kleiner, Hossein Mobahi, and Behnam Neyshabur. Sharpness-aware minimization for efficiently improving generalization. In *Proceedings of the International Conference on Learning Representations (ICLR)*, Virtual, May 2021.

Matt Fredrikson, Somesh Jha, and Thomas Ristenpart. Model inversion attacks that exploit confidence information and basic countermeasures. In *Proceedings of the ACM SIGSAC Conference on Computer and Communications Security (CCS)*, Denver Colorado, USA, October 2015.

Sheng Guo, Weilin Huang, Haozhi Zhang, Chenfan Zhuang, Dengke Dong, Matthew R Scott, and Dinglong Huang. Curriculumnet: Weakly supervised learning from large-scale web images. In *Proceedings of the European Conference on Computer Vision (ECCV)*, Munich, Germany, September 2018.

Roger Iyengar, Joseph P Near, Dawn Song, Om Thakkar, Abhradeep Thakurta, and Lun Wang. Towards practical differentially private convex optimization. In *Proceedings of the IEEE Symposium on Security and Privacy (SP)*, San Francisco, California, USA, May 2019.

Tsung-Yi Lin, Priya Goyal, Ross Girshick, Kaiming He, and Piotr Dollár. Focal loss for dense object detection. In *Proceedings of the IEEE International Conference on Computer Vision (ICCV)*, Venice, Italy, October 2017.

Jingcheng Liu and Kunal Talwar. Private selection from private candidates. In *Proceedings of the ACM SIGACT Symposium on Theory of Computing*, Phoenix, Arizona, USA, June 2019.

Yuzhe Ma, Xiaojin Zhu, and Justin Hsu. Data poisoning against differentially-private learners: Attacks and defenses. In *Proceedings of the International Joint Conference on Artificial Intelligence (IJCAI)*, Macao, China, August 2019.

Aditya Krishna Menon, Ankit Singh Rawat, Sashank J Reddi, and Sanjiv Kumar. Can gradient clipping mitigate label noise? In *Proceedings of the International Conference on Learning Representations (ICLR)*, New Orleans, Los Angeles, USA, May 2019.

Yurii Nesterov. *Introductory lectures on convex optimization: A basic course*, volume 87. Springer Science & Business Media, 2003.

Nicolas Papernot, Abhradeep Thakurta, Shuang Song, Steve Chien, and Úlfar Erlingsson. Tempered Sigmoid activations for deep learning with differential privacy. In *Proceedings of the Association for the Advancement of Artificial Intelligence (AAAI)*, Virtual, February 2021.

Md Atiqur Rahman, Tanzila Rahman, Robert Laganière, Noman Mohammed, and Yang Wang. Membership inference attack against differentially private deep learning model. *Transactions on Data Privacy*, 11(1):61–79, 2018.

Reza Shokri, Marco Stronati, Congzheng Song, and Vitaly Shmatikov. Membership inference attacks against machine learning models. In *Proceedings of the IEEE Symposium on Security and Privacy (SP)*, SAN JOSE, California, USA, May 2017.

Congzheng Song and Vitaly Shmatikov. Auditing data provenance in text-generation models. In *Proceedings of the ACM SIGKDD International Conference on Knowledge Discovery & Data Mining (KDD)*, Anchorage, Alaska, USA, August 2019.

Florian Tramèr and Dan Boneh. Differentially private learning needs better features (or much more data). In *Proceedings of the International Conference on Learning Representations (ICLR)*, Virtual, May 2021.

Wenxiao Wang, Tianhao Wang, Lun Wang, Nanqing Luo, Pan Zhou, Dawn Song, and Ruoxi Jia. DPlis: Boosting utility of differentially private deep learning via randomized smoothing. *Privacy Enhancing Technologies Symposium (PETS)*, 2021(4):163–183, 2021.

Yiru Wang, Weihao Gan, Jie Yang, Wei Wu, and Junjie Yan. Dynamic curriculum learning for imbalanced data classification. In *Proceedings of the IEEE International Conference on Computer Vision (ICCV)*, Seoul, Korea, October 2019.

Xi Wu, Fengan Li, Arun Kumar, Kamalika Chaudhuri, Somesh Jha, and Jeffrey Naughton. Bolt-on differential privacy for scalable stochastic gradient descent-based analytics. In *Proceedings of the ACM International Conference on Management of Data*, Chicago Illinois, USA, May 2017.

Da Yu, Huishuai Zhang, Wei Chen, Jian Yin, and Tie-Yan Liu. Gradient perturbation is underrated for differentially private convex optimization. In *Proceedings of the International Joint Conference on Artificial Intelligence (IJCAI)*, Yokohama, Japan, July 2020.

Da Yu, Huishuai Zhang, Wei Chen, and Tie-Yan Liu. Do not let privacy overbill utility: Gradient embedding perturbation for private learning. In *Proceedings of the International Conference on Learning Representations (ICLR)*, Virtual, May 2021.

Jiaqi Zhang, Kai Zheng, Wenlong Mou, and Liwei Wang. Efficient private ERM for smooth objectives. In *Proceedings of the International Joint Conference on Artificial Intelligence (IJCAI)*, Melbourne, Australia, August 2017.

Jingzhao Zhang, Tianxing He, Suvrit Sra, and Ali Jadbabaie. Why gradient clipping accelerates training: A theoretical justification for adaptivity. In *International Conference on Learning Representations (ICLR)*, New Orleans, Los Angeles, USA, May 2019.

Table 1: The architecture of end-to-end CNNs for Fashion-/MNIST (Papernot et al., 2021).

Layer	Parameters
Conv	16 filters of 8x8, stride 2, padding 2
MP	2x2, stride 1
Conv	32 filters of 4x4, stride 2, padding 0
MP	2x2, stride 1
FC	32 units
FC	10 units

Table 2: The architecture of end-to-end CNNs for CIFAR10 (Papernot et al., 2021).

Layer	Parameters
Conv x2	32 filters of 3x3, stride 1, padding 1
MP	2x2, stride 2
Conv x2	64 filters of 3x3, stride 1, padding 1
MP	2x2, stride 2
Conv x2	128 filters of 3x3, stride 1, padding 1
MP	2x2, stride 2
FC	128 units
FC	10 units

Table 3: The architecture of CNNs trained on top of public ScatterNet feature extractor for Fashion-/MNIST (Tramèr & Boneh, 2021).

Layer	Parameters
Conv	16 filters of 3x3, stride 2, padding 1
MP	2x2, stride 1
Conv	32 filters of 3x3, stride 1, padding 1
MP	2x2, stride 1
FC	32 units
FC	10 units

Table 4: The architecture of CNN trained on top of public ScatterNet feature extractor for CIFAR10 (Tramèr & Boneh, 2021).

Layer	Parameters
Conv x2	64 filters of 3x3, stride 1, padding 1
MP	2x2, stride 2
Conv x2	64 filters of 3x3, stride 1, padding 1
MP	2x2, stride 2
FC	10 units

A CLASSIFIERS

Table 1 and Table 2 show the architecture of end-to-end CNNs for MNIST, FashionMNIST and CIFAR10, suggested by Papernot et al. (2021). Table 3 and Table 4 show the architecture of CNNs trained on ScatterNet features for MNIST, FashionMNIST and CIFAR10, suggested by Tramèr & Boneh (2021).

B HYPERPARAMETERS

Table 5 reports hyperparameter values of the DP-SGD configuration across all approaches, suggested by Tramèr & Boneh (2021). Table 6 reports the hyperparameter values of our proposed loss function, obtained through a hyperparameter search on values reported in Table 7.

Table 5: Training hyperparameter values obtained through line search Tramèr & Boneh (2021).

Dataset	Learning rate	Momentum	Batch size	Epochs	Noise scale	Clipping norm
End-to-end CNN						
CIFAR10	1	0.9	1024	30	1.54	0.1
Fashion-MNIST	4	0.9	2048	40	2.15	0.1
MNIST	0.5	0.9	512	40	1.23	0.1
CNN trained on ScatterNet features						
CIFAR10	4	0.9	8192	60	5.67	0.1
Fashion-MNIST	4	0.9	2048	40	2.15	0.1
MNIST	1	0.9	1024	25	1.35	0.1

Table 6: The value of the hyperparameter of our loss function.

	CIFAR10	FashionMNIST	MNIST
`O-T-CNN`	$e_t = 7, \beta = 11, \gamma = 5$	$e_t = 0, \beta = 1, \gamma = 5$	$e_t = 0, \beta = 1, \gamma = 5$
`O-T-PFE_CNN`	$e_t = 2, \beta = 1, \gamma = 2$	$e_t = 2, \beta = 51, \gamma = 2$	$e_t = 2, \beta = 11, \gamma = 10$

Table 7: Hyperparameters for our proposed loss function.

Parameter	Value
e_t	Start=0, End=10, Step-size=1
β	Start=1, End=200, Step-size=10

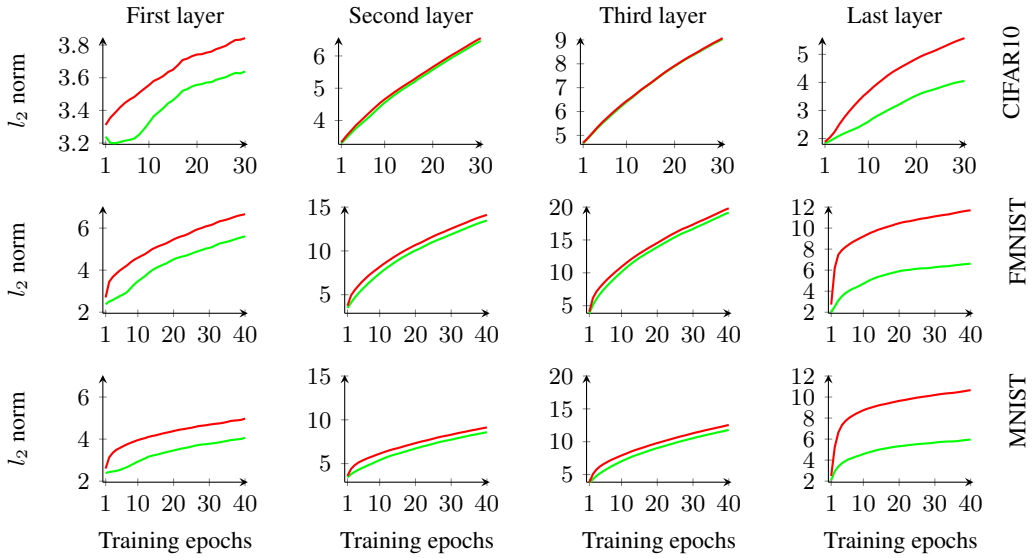

Figure 10: l_2 norm of model weights in CE−T−CNN (——) and O−T−CNN (——) using CIFAR10, FashionMNIST and MNIST.

C l_2 NORM OF PRE-ACTIVATION AND WEIGHTS

Figure 10 and Figure 11 show the l_2 norm of weights and pre-activation of models trained by DP-SGD approaches on CIFAR10, FashionMNIST and MNIST.

D CONFUSION MATRICES OF PER-CLASS ACCURACY

Figure 12 visualises the confusion matrices of per-class training accuracy for non-private learning with SGD, private learning with the CE−T−CNN baseline, and private learning with our approach O−T−CNN using CIFAR10, FashionMNIST and MNIST.

E PER-EXAMPLE GRADIENTS

Figure 13 provides the histogram of per-example gradient l_2 norms in CE−T−CNN and O−T−CNN on CIFAR10, FashionMNIST and MNIST.

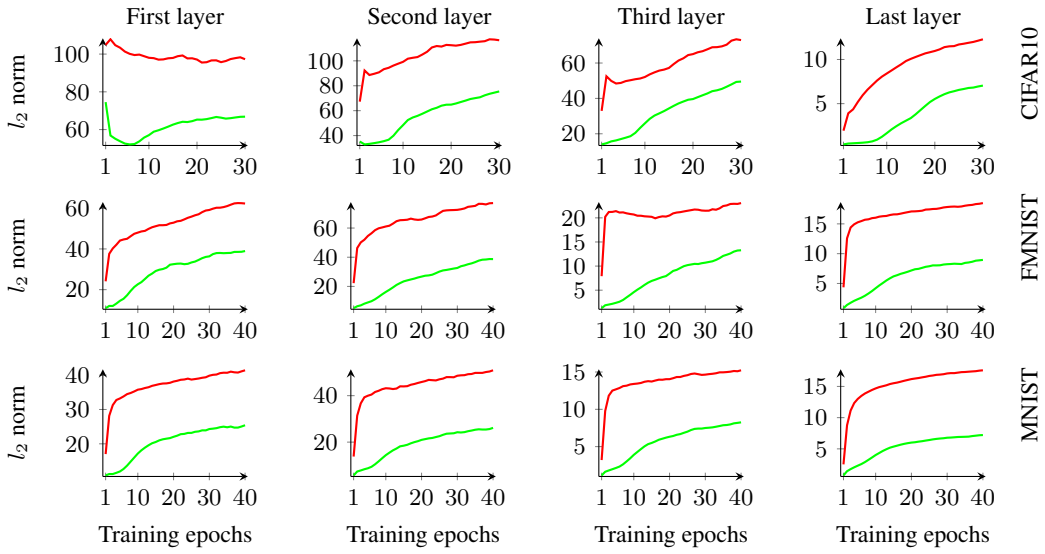

Figure 11: Pre-activation l_2 norm per layer of CE−T−CNN (——) and O−T−CNN (——) on CIFAR10, FashionMNIST and MNIST.

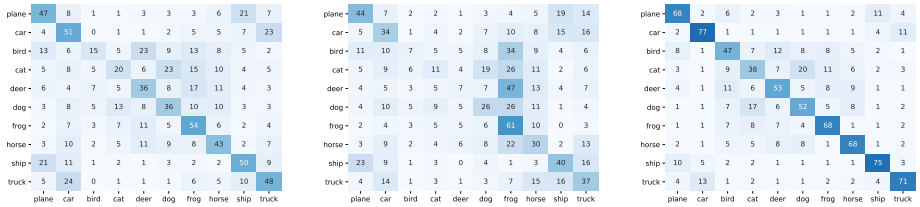

a) Initial epoch 2 in CIFAR10

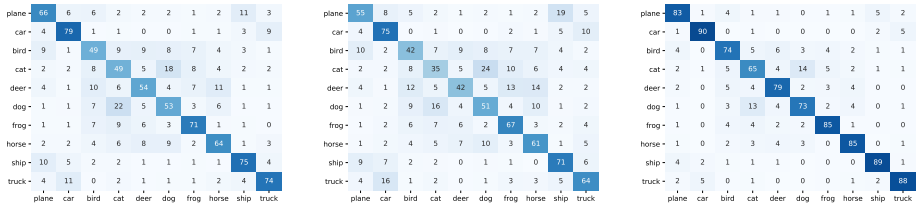

b) Late epoch 20 in CIFAR10

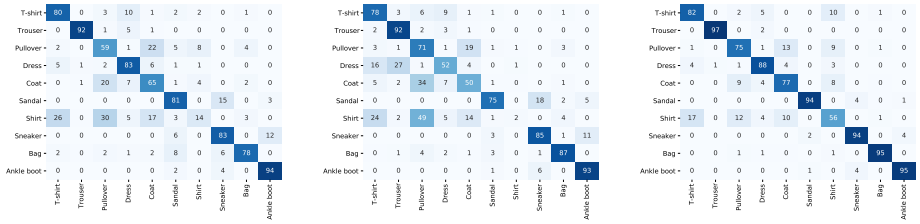

c) Initial epoch 2 in FashionMNIST

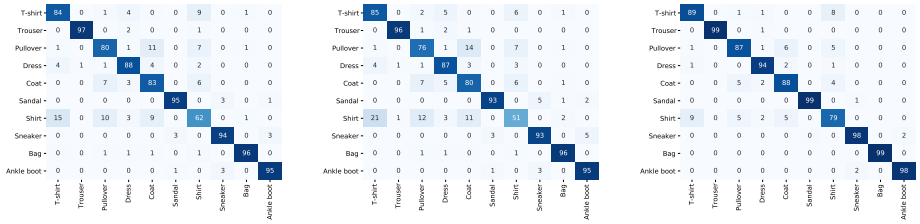

d) Late epoch 20 in FashionMNIST

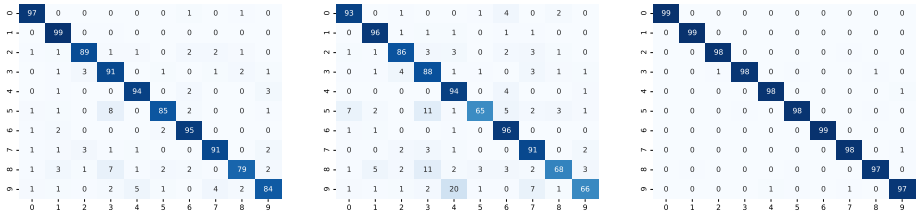

e) Initial epoch 2 in MNIST

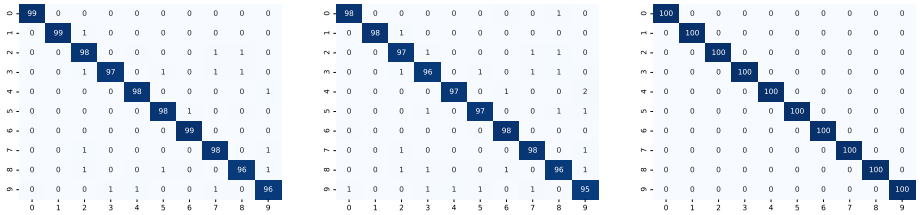

f) Late epoch 20 in MNIST

Figure 12: Confusion matrices that show per-class training accuracy of `O-T-CNN` (first column), `CE-T-CNN` (second columns) and non-private SGD approach (last columns) using CIFAR10, FashionMNIST and MNIST.

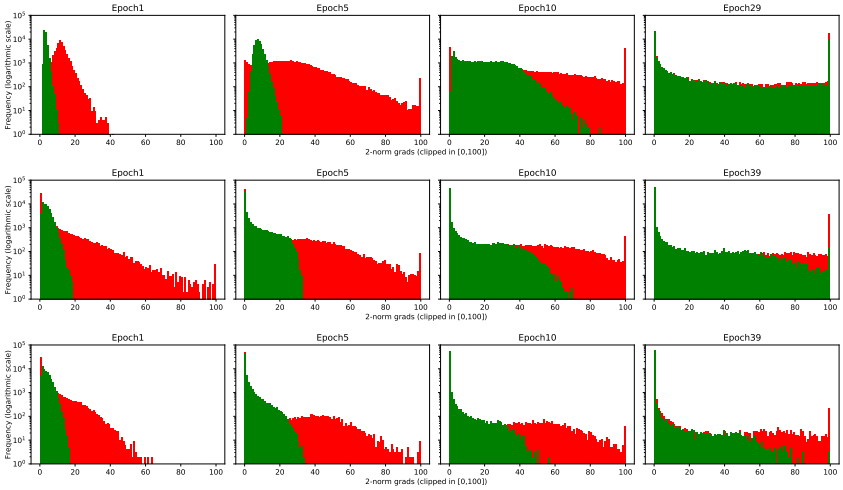

Figure 13: Histogram of l_2 norm of per-example gradient in CE−T−CNN and O−T−CNN on CIFAR10 (top row), FashionMNIST (middle row) and MNIST (bottom row).